



Poly(ADP-ribose) polymerase inhibitors attenuate necrotic but not apoptotic neuronal death in experimental models of cerebral ischemia

F Moroni^{*1}, E Meli¹, F Peruginelli¹, A Chiarugi¹, A Cozzi¹,
R Picca¹, P Romagnoli², R Pellicciari³ and
DE Pellegrini-Giampietro¹

¹ Dipartimento di Farmacologia Preclinica e Clinica, Università di Firenze,
Firenze, Italy

² Dipartimento di Anatomia, Istologia e Medicina Legale, Università di Firenze,
Firenze, Italy

³ Dipartimento di Chimica e Tecnologia del Farmaco, Università di Perugia,
Perugia, Italy

* Corresponding author: F Moroni, Dipartimento di Farmacologia Preclinica e
Clinica, Viale G. Pieraccini 6, I-50139 Firenze, Italy.
Tel: +39-055-4271-266; Fax: +39-055-4271-280;
E-mail: fmoroni@pharm.unifi.it

Received 17.1.01; revised 8.3.01; accepted 30.3.01
Edited by F Miller

Abstract

An excessive activation of poly(ADP-ribose) polymerase (PARP) has been proposed to play a key role in post-ischemic neuronal death. We examined the neuroprotective effects of the PARP inhibitors benzamide, 6(5H)-phenanthridinone, and 3,4-dihydro-5-[4-1(1-piperidinyl)butoxy]-1(2H)-isoquinolinone in three rodent models of cerebral ischemia. Increasing concentrations of the three PARP inhibitors attenuated neuronal injury induced by 60 min oxygen-glucose deprivation (OGD) in mixed cortical cell cultures, but were unable to reduce CA1 pyramidal cell loss in organotypic hippocampal slices exposed to 30 min OGD or in gerbils following 5 min bilateral carotid occlusion. We then examined the necrotic and apoptotic features of OGD-induced neurodegeneration in cortical cells and hippocampal slices using biochemical and morphological approaches. Cortical cells exposed to OGD released lactate dehydrogenase into the medium and displayed ultrastructural features of necrotic cell death, whereas no caspase-3 activation nor morphological characteristics of apoptosis were observed at any time point after OGD. In contrast, a marked increase in caspase-3 activity was observed in organotypic hippocampal slices after OGD, together with fluorescence and electron microscope evidence of apoptotic neuronal death in the CA1 subregion. Moreover, the caspase inhibitor Z-VAD-FMK reduced OGD-induced CA1 pyramidal cell loss. These findings suggest that PARP overactivation may be an important mechanism leading to post-ischemic neurodegeneration of the necrotic but not of the apoptotic type. *Cell Death and Differentiation* (2001) 8, 921–932.

Keywords: neuroprotection; apoptosis; necrosis; oxygen-glucose deprivation

Abbreviations: DIV, days *in vitro*; DPQ, 3,4-dihydro-5-[4-1(1-piperidinyl)butoxy]-1(2H)-isoquinolinone; HBSS, Hanks' balanced salt solution; LDH, lactate dehydrogenase; MEM, minimal essential medium; MS, medium stock; NBQX, 6-nitro-7-sulphamoylbenzof[quinoxaline-2,3-dione; OGD, oxygen-glucose deprivation; PAR, poly(ADP-ribose); PARP, poly(ADP-ribose) polymerase; PI, propidium iodide; PND, 6(5H)-phenanthridinone; TdT, terminal deoxynucleotidyl transferase; Z-VAD-FMK, carbon-benzyloxy-valyl-alanyl-aspartyl-[O-methyl]-fluoromethylketone

Introduction

A pivotal role in the pathogenesis of neuronal death following cerebral ischemia is played by the massive release of excitotoxic glutamate and the excessive stimulation of ionotropic and metabotropic glutamate receptors.^{1–6} Post-ischemic injury is also exacerbated by the increased formation of free radicals, which is known to act in concert with glutamate receptor activation and cooperates in the genesis and propagation of neuronal damage.^{7,8} A mechanism whereby stimulation of glutamate receptors may lead to neuronal loss involves the activation of free radical generating enzymes, the formation of reactive species (including NO) that damage DNA,⁹ and overactivation of poly(ADP-ribose) polymerase (PARP; EC 2.4.2.30).^{10,11}

PARP, a nuclear enzyme also known as poly(ADP-ribose) synthetase or poly(ADP-ribose) transferase, has recently emerged as a key player in the mechanisms leading to cell death. PARP is activated by DNA strand breaks and catalyzes the attachment of chains of poly(ADP-ribose) (PAR) from its substrate NAD to a variety of nuclear proteins, including PARP itself.¹² When DNA damage is mild, PARP is thought to be involved in the maintenance of chromatin integrity. Conversely, overactivation of PARP in response to massive DNA damage has been proposed to play a 'suicidal role',^{13–15} due to the marked depletion of NAD tissue stores and the resultant decrease in the rate of glycolysis, electron transport and ATP formation. When poly(ADP-ribose)ylation is excessive, ATP is also consumed in attempts to regenerate NAD, eventually leading to cell death from disruption of oxidative metabolism.^{16–18} According to this view, glutamate has been shown to increase PAR immunoreactivity in cerebellar granule cells,¹⁰ and a dramatic PAR formation and loss of NAD is observed following focal ischemia in rodents.^{19–21} In addition, PARP inhibitors attenuate excitotoxicity *in vitro*^{10,11} and the infarct volume following middle cerebral artery occlusion *in vivo*.^{19,20,22,23} Finally, targeted deletion

of the PARP gene provides substantial neuroprotection in the same experimental models.^{19,24}

Benzamide, 6(5H)-phenanthridinone (PND), and 3,4-dihydro-5-[4-(1-piperidinyl)butoxy]-1(2H)-isoquinolinone (DPQ) are three PARP inhibitors with increasing degrees of potency and selectivity^{25,26} that have been previously utilized in a number of experimental studies.¹⁶ We herein examine the neuroprotective effects of these agents in three different models of cerebral ischemia. In addition, in order to understand whether there is a correlation between PARP overactivation and the pattern of cell death we characterize the necrotic and apoptotic features of neurodegeneration induced by oxygen-glucose deprivation (OGD).

Results

Benzamide, PND and DPQ inhibit PARP activity *in vitro*

Benzamide, PND and DPQ inhibited PARP activity in a dose-dependent manner when tested in an *in vitro* assay system (Figure 1). Consistent with previous findings,^{25,26} PND and

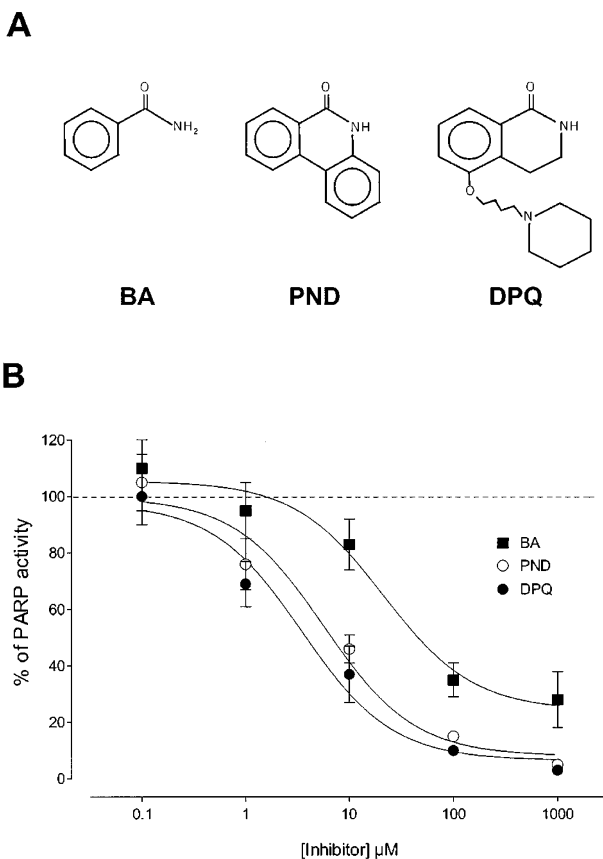


Figure 1 (A) Molecular structures of the three PARP inhibitors used in the present study: benzamide (BA), 3,4-dihydro-5-[4-(1-piperidinyl)butoxy]-1(2H)-isoquinolinone (DPQ), and 6(5H)-phenanthridinone (PND). (B) Inhibition of PARP activity in partially purified enzyme preparations by BA, PND and DPQ. Each point is the mean \pm S.E.M. of at least three experiments conducted in triplicate. See text for experimental details

DPQ were more potent inhibitors than benzamide. The IC₅₀ values for their effects were 30 ± 4 μM for benzamide, 5.7 ± 0.2 μM for PND and 3.5 ± 0.5 μM for DPQ.

PARP inhibitors protect cortical neurons against OGD injury

Exposure of mixed cortical cells to a high concentration (1 mM) of glutamate for 24 h induced a maximal degree of neuronal death. Phase-contrast microscopy revealed that virtually all neuronal cell bodies were damaged, whereas the underlying glial layer was not affected.⁶ Complete neuronal death induced by 24 h exposure to glutamate was associated with a substantial (approximately fourfold the basal levels) efflux of lactate dehydrogenase (LDH) into the bathing medium. Exposure to OGD for 60 min produced an intermediate level of neuronal damage, as detected qualitatively by fluorescence microscopy in cells incubated with propidium iodide (PI) or quantitatively by measuring the release of LDH into the medium (Figure 2A). The release of LDH evoked by 60 min OGD was $74 \pm 6\%$ of that observed by exposing the cultures to 1 mM glutamate for 24 h.

OGD neurotoxicity was attenuated in a dose-dependent manner when the PARP inhibitors benzamide, PND and DPQ were added to the incubation medium during the 60 min OGD challenge and the subsequent 24 h recovery period (Figure 2A). Significant neuroprotection was observed with 500 μM benzamide, 100 μM PND and 10 μM DPQ. The maximal degree of neuroprotection achieved with PARP inhibitors was comparable to that previously observed, in the same experimental protocol, with antagonists of ionotropic or group I metabotropic glutamate receptors.^{6,27} DPQ at 10 μM proved to be neuroprotective also when added immediately or 30 min after the termination of OGD (Figure 2B).

PARP inhibitors do not protect organotypic hippocampal slices against OGD injury

When hippocampal slices incubated with PI were exposed to glutamate, fluorescence levels increased dramatically in virtually all neuronal populations.⁶ Maximal damage was achieved in this system by exposing the slices to 10 mM glutamate for 24 h. Exposure to OGD for 30 min caused a fluorescence pattern in which PI staining was more intense in the CA1 area.^{6,27} Quantitative analysis carried out in the hippocampal CA1 subregion 24 h after the insult revealed that 30 min OGD produced PI fluorescence levels that were $72 \pm 4\%$ of those observed when neuronal injury was maximal (Figure 3A).

Although ionotropic and group I metabotropic glutamate receptor antagonists were previously shown to attenuate CA1 injury in this experimental model,^{6,27} PND (10–100 μM, the use of higher doses was precluded by the toxicity of the vehicle) and DPQ (10–300 μM) failed to reduce the extent of OGD-induced neuronal death when added to the incubation medium during the 30 min insult and the subsequent 24 h recovery period (Figure 3A). Only benzamide among PARP inhibitors displayed a mild degree of neuroprotection, but this effect was not significant.

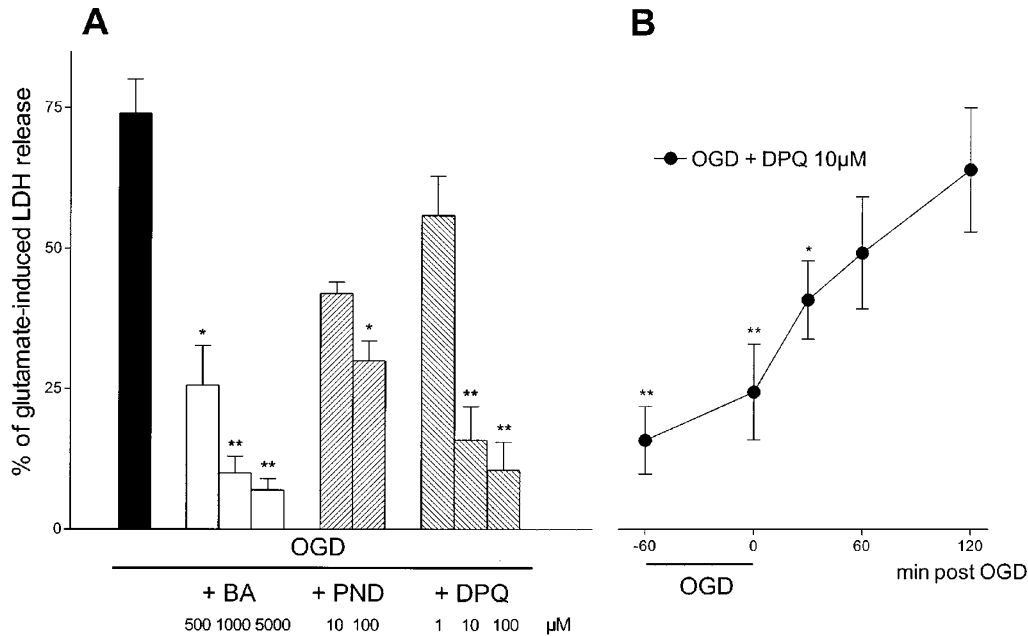


Figure 2 Benzamide, PND, and DPQ protect against OGD neurotoxicity in murine cortical cells. Mixed cortical cultures were exposed to 60 min OGD and 24 h neuronal death was assessed by measuring the release of LDH in the medium. Data are expressed as per cent of maximal damage, as produced by exposure to 1 mM glutamate for 24 h. Background LDH release was determined in control sister cultures not exposed to OGD and was subtracted from all experimental values. (A) Neuronal death was significantly reduced by addition of 0.5–5 mM benzamide (BA), 100 µM PND, or 10–100 µM DPQ to the incubation medium during OGD exposure and the subsequent 24 h recovery period. Each bar represents the mean ± S.E.M. of at least five experiments. (B) DPQ was neuroprotective also when added during or at 0 and 30 min after OGD. Each point represents the mean ± S.E.M. of at least three experiments. * $P < 0.05$ and ** $P < 0.01$ vs OGD alone (ANOVA + Tukey's *w*-test)

PARP inhibitors do not protect CA1 pyramidal cells following global ischemia in gerbils

Seven days following transient bilateral carotid occlusion in gerbils, histological examination of hippocampal sections revealed that almost all ($91 \pm 2\%$) pyramidal cells in the CA1 region were selectively and severely damaged (Figure 3B). Intraperitoneal administration of the AMPA receptor antagonist 6-nitro-7-sulphamoylbenzo[f]quinoxaline-2,3-dione (NBQX) (30 mg/Kg) at 0, 15 and 30 min following reperfusion induced a dramatic attenuation of post-ischemic cell loss (Figure 3B), in confirmation of Sheardown *et al.*²⁸ Similar neuroprotective results were previously obtained using a glycine antagonist and free radical scavenger,²⁹ kynurenine hydroxylase inhibitors,³⁰ or group I metabotropic glutamate receptor antagonists.^{6,27} Figure 3B shows that benzamide and DPQ were unable to improve the survival of CA1 pyramidal cells following global ischemia in the gerbil. Both PARP inhibitors were administered using doses and multiple i.p. injection paradigms that are known to result in brain drug concentrations that are both effective in inhibiting PARP activity and neuroprotective in mice and rats.^{22,31,32}

Characterization of neuronal death in cortical cell cultures exposed to OGD

Both necrotic and apoptotic neuronal death have been described following cerebral ischemia.^{33–35} In order to understand whether there was a correlation between the results observed with PARP inhibitors and the pattern of cell

death, we examined the necrotic and apoptotic features of OGD-induced neurodegeneration in our *in vitro* experimental models using biochemical and morphological approaches.

The activation of caspase-3 has a central and exclusive role in the initiation and the execution of neuronal apoptosis.³⁶ We therefore examined caspase-3-like activity in cortical cultures exposed to OGD and to conditions that are known to induce either necrotic or apoptotic neuronal death. Exposure of cortical neurons to an intense excitotoxic insult such as 1 mM glutamate for 24 h induced complete neuronal death and massive release of LDH but no activation of caspase-3 (Table 1), indicating that the type of cell death was necrotic.³⁷ In contrast, continuous application of the nonselective protein kinase C inhibitor staurosporine (100 nM) is known to cause apoptotic neuronal death in this system,³⁸ as confirmed by the marked increase in caspase-3 activity that was detected 24 h later (Table 1). Exposure of cortical cells to 60 min OGD induced a time-dependent efflux of LDH into the medium that was highest 24 h after the insult (data not shown). However, no significant activation of caspase-3 could be observed at any time point following OGD (Table 1), suggesting that the involvement of apoptosis in OGD-induced neuronal death in this model is modest.

Morphological analysis of cortical cells exposed to the same experimental conditions supported this idea. Fluorescence microscopy of cultures stained with the nuclear dye Hoechst 33258 revealed typical apoptotic chromatin fragmentation only when cells were treated with 100 nM staurosporine for 24 h (Figure 4B). Apoptotic chromatin

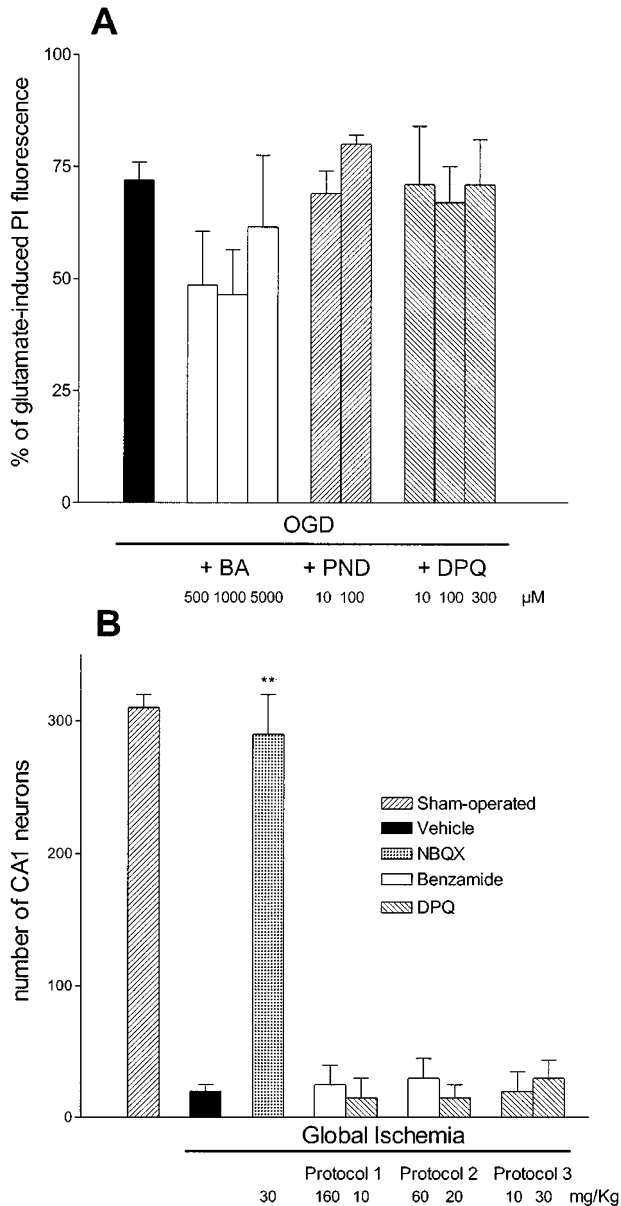


Figure 3 Benzamide, PND and DPQ do not attenuate CA1 damage produced by OGD in organotypic hippocampal slices (A) or by transient global ischemia in gerbils (B). (A) Hippocampal slices were exposed to 30 min OGD and 24 h later CA1 damage was assessed by measuring the intensity of PI fluorescence. Data are expressed as per cent of maximal neuronal death, as measured following application of 10 mM glutamate for 24 h. Background fluorescence was determined in control sister cultures not exposed to OGD and was subtracted from all experimental values. Neuronal death in CA1 was not attenuated when benzamide (BA, 0.5–5 mM), PND (10–100 μM) or DPQ (10–300 μM) were added during OGD and the 24 h recovery period. Each bar represents the mean ± S.E.M. of at least six experiments. (B) Gerbils were subjected to 5 min bilateral carotid occlusion and 7 days later CA1 pyramidal cell death was assessed by morphological criteria. NBQX (30 mg/Kg) was administered i.p. at 0, 15 and 30 min after reperfusion. *Protocol 1*, benzamide (160 mg/Kg) or DPQ (10 mg/Kg) were administered i.p. 2 h before bilateral carotid occlusion. *Protocol 2*, benzamide (60 mg/Kg) or DPQ (20 mg/Kg) were administered i.p. at 0, 15 and 30 min after reperfusion. *Protocol 3*, DPQ (10 or 30 mg/Kg) was administered i.p. at 0, 60, 180 and 360 min after reperfusion. Data are expressed as the number of normal pyramidal cells counted in the CA1 subfield. Administration of 30 mg/kg NBQX i.p. induced dramatic neuroprotection but none of the benzamide or DPQ administration protocols reduced CA1 pyramidal cell loss. Each bar represents the mean ± S.E.M. of at least five animals. ** $P < 0.01$ vs vehicle (ANOVA + Tukey's w -test)

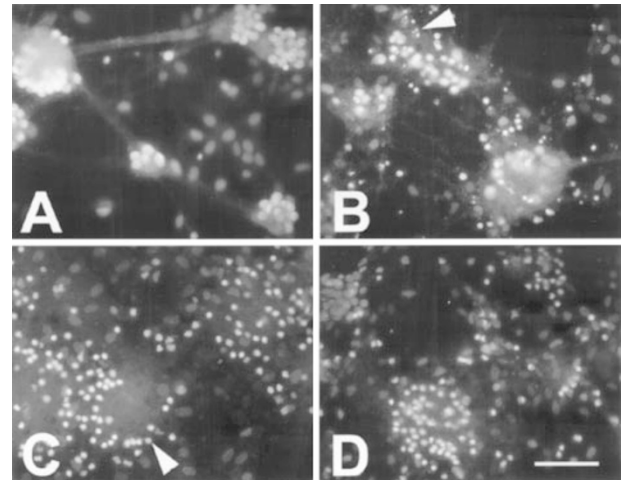


Figure 4 Murine cortical cells exposed to OGD do not undergo apoptotic chromatin fragmentation. Cultures were exposed to 100 nM staurosporine, 1 mM glutamate or 60 min OGD, incubated with the nuclear dye Hoechst 33258, and then photographed under fluorescence optics. (A) Clusters of cortical neurons under control conditions, displaying dispersed chromatin. Scattered glial cells in the underlying layer can be detected between clusters. (B) Neurons exposed to 100 nM staurosporine for 24 h, exhibiting apoptotic nuclear fragmentation (arrowhead). (C) Neurons exposed to 1 mM glutamate for 24 h, showing small, brilliant and round-shaped nuclei (arrow) but no fragmentation, indicative of necrotic cell death. (D) Neurons exposed to 60 min OGD and observed later, displaying cell death of the necrotic type. No chromatin fragmentation can be detected. Bar = 50 μm

fragmentation could not be observed when 1 mM glutamate was present in the medium for 24 h, but virtually all neurons displayed round, small, and highly refringent nuclei, which is suggestive of necrotic cell death (Figure 4C). In cultures exposed to 60 min OGD, neuronal death was massive but devoid of apoptotic nuclear fragmentation 24 h later (Figure 4D). Electron microscopy revealed typical features of necrotic neuronal death in cultured cortical cells examined 6 h after exposure to 60 min OGD (Figure 5). Neurons displayed nuclear and plasma membrane breaks (Figure 5B–D), large vacuoles as well as swollen mitochondria and organelles in a dispersed cytoplasm (Figure 5C and D), and irregularly clumped chromatin (Figure 5D). Apoptotic signs of neurodegeneration could not be found. At the later time-point examined (24 h after OGD) almost all neuronal cells were replaced by debris and cellular residues, but no apparent signs of degeneration were observed in glial cells (Figure 5E).

Characterization of neuronal death in organotypic hippocampal slices exposed to OGD

Incubation of organotypic hippocampal slices with relatively large concentrations (10 μM) of staurosporine for 24 h caused a 2.6-fold increase in caspase-3 activity, as compared with control cultures (Table 1). Similarly to what was observed in cortical cell cultures, an intense excitotoxic insult (10 mM glutamate for 24 h) induced massive neuronal injury but no activation of caspase-3. In this model however, 30 min exposure to OGD led to a marked and time-dependent increase in caspase-3 activity that was prevented by the

Table 1 Caspase-3 is activated in organotypic hippocampal slices but not in murine cortical cultures exposed to OGD

	Cortical cells		Hippocampal slices	
	pmol/10 ⁶ cells	(%)	pmol/slice	(%)
Basal	16.1 ± 2.5	(23)	46.9 ± 5.0	(38)
Staurosporine	70.1 ± 11.1**	(100)	123.5 ± 5.2**	(100)
Glutamate	15.1 ± 1.1	(21)	40.0 ± 3.0	(33)
3 h after OGD	18.8 ± 7.0	(27)	72.5 ± 4.2**	(59)
6 h after OGD	28.7 ± 12.0	(41)	87.8 ± 4.3**	(71)
24 h after OGD (A)	24.0 ± 2.8	(34)	95.3 ± 3.2**	(77)
A + 100 μM Z-VAD-FMK	21.3 ± 4.9	(30)	75.4 ± 8.2	(61)
A + 300 μM Z-VAD-FMK	25.4 ± 2.6	(36)	59.6 ± 7.3#	(48)

Murine cortical cultures were exposed to 1 mM glutamate or 100 nM staurosporine for 24 h and to OGD for 60 min, whereas organotypic hippocampal slices were exposed to 10 mM glutamate or 10 μM staurosporine for 24 h and to OGD for 30 min. Z-VAD-FMK was present in the medium during the OGD insult and the subsequent 24 h recovery period. Caspase-3 activity was measured in the supernatant of lysed and spun cell or slice cultures after glutamate or staurosporine incubation or at the indicated period after OGD. Data are expressed as pmoles of fluorescent rhodamine 110/10⁶ cortical cells or hippocampal slice, and represent the mean ± S.E.M. of at least four experiments. Staurosporine but not glutamate induced a marked increase in caspase-3 activity in both systems, whereas OGD induced a time-dependent, Z-VAD-FMK-sensitive, increase in caspase-3 activity only in hippocampal slices. ***P* < 0.01 vs basal; #*P* < 0.05 vs A (ANOVA + Tukey's *w*-test)

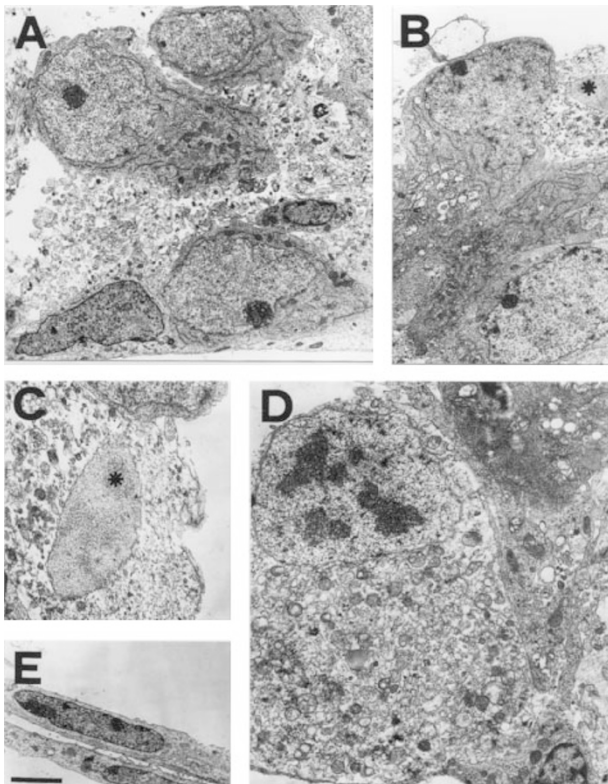


Figure 5 Electron microscope evidence for necrotic cell death in murine cortical cultures exposed to 60 min OGD. (A) Control healthy neurons showing nuclei with dispersed chromatin and a clearly defined nucleolus. A glial cell can be detected at the bottom-left corner of the microphotograph. (B) Six h after OGD, two well preserved neurons together with a shrunken, damaged neuron (asterisk). (C) Enlarged microphotograph of the same damaged neuron shown in B, rotated clockwise by 90° with the asterisk in the same position, displaying signs of necrotic degeneration. Chromatin is condensing, the nuclear and plasma membranes are disrupted, the cytoplasm is dispersed and contains vacuoles and swollen organelles. (D) Another enlarged neuron observed 6 h after 60 min OGD, showing necrotic features such as clumped chromatin, amorphous organelles, mitochondrial densities and cytoplasm disorganization. (E) Twenty-four h after 60 min OGD, only healthy and isolated glial cells can be detected. Bar = 2 μm in A, B and D and 1 μm in C and E

caspase inhibitor carbonbenzoxy-valyl-alanyl-aspartyl-[O-methyl]-fluoromethylketone (Z-VAD-FMK) (300 μM, Table 1), suggesting that apoptosis may contribute to OGD-induced neuronal death in organotypic hippocampal slices. Accordingly, 100 and 300 μM Z-VAD-FMK reduced (by 19 and 44%, respectively) the OGD-induced increase in CA1 PI fluorescence when added to the incubation medium during the 30 min OGD insult and the subsequent 24 h recovery period (Table 2).

Morphological analysis of hippocampal slices stained with Hoechst 33258 confirmed this view by revealing that OGD was able to induce apoptotic condensation and fragmentation of chromatin in the CA1 subregion (Figure 6D). The number of apoptotic pyramidal cells was dramatically increased in hippocampal CA1 when cultures were exposed for 24 h to 10 μM staurosporine (set as 100% of apoptotic cells), was at control levels 24 h after exposure to 10 mM glutamate (8% of apoptotic cells), and was at intermediate but significantly increased levels (45% of apoptotic cells) 3 and 24 h after exposure to 30 min OGD (Table 3). Staurosporine, but not OGD, was able to promote the appearance of apoptotic cells in other areas of the hippocampus, including the CA3 region (data not shown). The density of apoptotic cells in the CA1 region of hippocampal slices, as detected by the fluorescent FragEL DNA Fragmentation Detection Kit, was dramatically increased 24 h after OGD (Figure 6F). Electron microscopy revealed typical characteristics of apoptotic neuronal death in hippocampal slices exposed to OGD (Figure 7). Six h after OGD, some neurons appeared normal (Figure 7B), but others displayed typical features of apoptosis, including clumped chromatin, a darkened cytoplasm with vacuoles, and membrane preservation (Figure 7C). Many neurons were damaged 24 h after OGD, displaying variable degrees of apoptotic degeneration (Figure 7D) or apoptotic bodies surrounded by glial cell processes (Figure 7E).

Discussion

Our results show that the PARP inhibitors benzamide, PND and DPQ dose-dependently attenuate OGD-induced neuro-

Table 2 The caspase inhibitor Z-VAD-FMK reduces CA1 pyramidal cell death in organotypic hippocampal slices exposed to OGD

	Cortical cells		Hippocampal slices	
	LDH release (units/L)	(%)	PI fluorescence (mean ± S.E.M.)	(%)
Glutamate	418 ± 33*	(100)	136 ± 6**	(100)
24 h after OGD	310 ± 25	(74)	98 ± 5	(72)
OGD + 100 μM Z-VAD-FMK	291 ± 42	(70)	79 ± 7*	(58)
OGD + 300 μM Z-VAD-FMK	298 ± 36	(71)	65 ± 8**	(48)

Murine cortical cultures were exposed to 1 mM glutamate for 24 h and to OGD for 60 min, whereas organotypic hippocampal slices were exposed to 10 mM glutamate for 24 h and to OGD for 30 min. Z-VAD-FMK was present in the medium during the OGD insult and the subsequent 24 h recovery period. Data for cortical cells are expressed as units of LDH/L minus background (left, see legend to Figure 2) and as a percentage of 1 mM glutamate-induced neuronal injury (right). Data for hippocampal slices are expressed as CA1 PI fluorescence 24 h after glutamate or OGD exposure minus the background fluorescence as detected in control slices ($F_{24} - F_B$, left, see Materials and Methods) and as a percentage of 10 mM glutamate-induced neuronal injury (right). Values represent the mean ± S.E.M. of at least four experiments. * $P < 0.05$ and ** $P < 0.01$ vs OGD (ANOVA + Tukey's *w*-test)

Table 3 Number of apoptotic cells in the CA1 region of organotypic hippocampal slices

	Number of apoptotic cells/field	%	n (slices)
Control	0.7 ± 0.2	3	14
Staurosporine	21.8 ± 3.1**	100	6
Glutamate	1.8 ± 0.3	8	8
3 h after OGD	9.8 ± 2.0*	45	6
24 h after OGD	9.9 ± 1.3*	45	14

Apoptotic nuclei (displaying fragmented chromatin) were revealed by Hoechst 33258 staining, counted in three CA1 fields per slice, averaged, and expressed as mean ± S.E.M. number of apoptotic cells per field. Twenty-four h exposure to 10 μM staurosporine, but not to 10 mM glutamate, induced a maximal increase in the number of apoptotic cells. Three and 24 h after exposure to 30 min OGD, an intermediate but significant increase in the number of apoptotic cells was detected. * $P < 0.05$ and ** $P < 0.01$ vs control (ANOVA + Tukey's *w*-test)

nal injury in mixed cortical cultures but fail to reduce hippocampal CA1 pyramidal cell loss in organotypic hippocampal slice cultures exposed to OGD or in gerbils following transient global ischemia. DPQ was neuroprotective in cortical cultures even when added up to 30 min after the OGD insult was terminated. Whereas OGD induced mostly necrotic neuronal death in cortical cultures, CA1 pyramidal cells of organotypic slices exposed to OGD displayed biochemical and morphological signs of apoptotic neurodegeneration. These findings suggest that PARP overactivation may be an important mechanism leading to post-ischemic neurodegeneration of the necrotic but not of the apoptotic type.

Our neuroprotection data corroborate and extend previous observations showing that benzamide and DPQ reduce neuronal death in cortical cultures exposed to OGD.²⁴ PARP inhibitors have also been demonstrated to attenuate excitotoxic damage *in vitro*^{10,11} and the infarct size following middle cerebral artery occlusion in mice¹⁹ and rats,^{20,22,23} even when administered up to 30 min post-ischemia.²¹ The involvement of PARP activation in neuronal death following excitotoxicity and focal ischemia is further substantiated by the resistance to these types of insults observed in PARP gene-deleted mice^{19,24} and by the finding that the increased PAR immunoreactivity observed in focal ischemic animals is reduced by treatment with PARP inhibitors.^{19–21} Nevertheless, inhibition of PARP is not a universal protective strategy. Our results show that concentrations of PARP inhibitors that

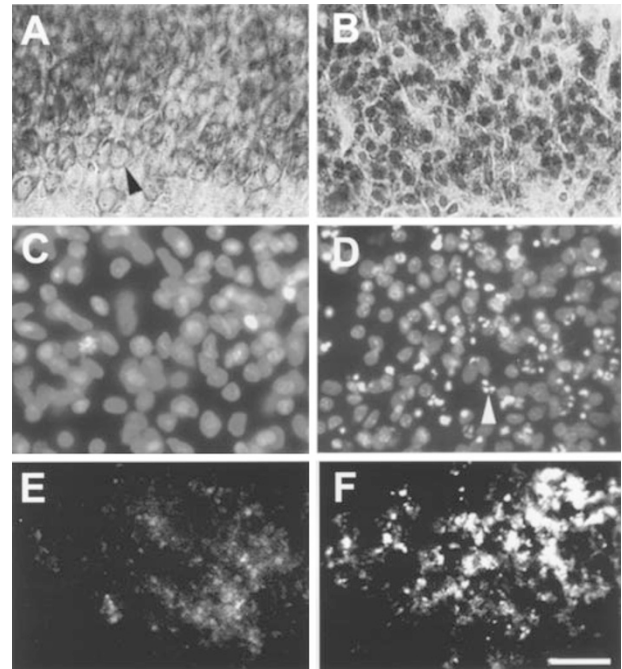


Figure 6 Organotypic hippocampal slices exposed to OGD undergo apoptotic chromatin fragmentation. (A, B) Cultures were exposed for 30 min to normoxic (A) or OGD (B) conditions, fixed 24 h later with 4% paraformaldehyde, and then stained with toluidine blue. Under bright-field microscope observation, histologically normal CA1 pyramidal cells (arrowhead) can be recognized in (A), whereas OGD-injured neurons displayed a shrunken and dark staining nucleus (B). (C, D) Cultures were exposed for 30 min to normoxic (C) or OGD (D) conditions, stained 24 h later with the nuclear dye Hoechst 33258, and then photographed under fluorescence optics. Control pyramidal cells in the CA1 area under normoxic conditions are shown in (C). CA1 pyramidal cells exposed to OGD (D), displayed extensive apoptotic nuclear fragmentation (arrowhead). (E, F) Cultured slices were exposed for 30 min to normoxic (E) or OGD (F) conditions, labeled 24 h later using the Fluorescein-FragEL DNA Fragmentation Detection Kit, and photographed under fluorescence optics. The intensity of DNA end-labeling with fluorescent deoxynucleotides catalyzed by TdT was markedly increased in the CA1 area of slices to OGD (F) as compared to background fluorescence under normoxic conditions (E). Bar = 35 μm (A–D) and 50 μm (E, F)

reduce OGD injury in cortical cells are without effect in organotypic hippocampal slices, and that administration paradigms of benzamide and DPQ previously shown to be neuroprotective in rodents^{22,31} do not prevent delayed CA1 pyramidal cell death in the gerbil model of global ischemia. These negative results are in line with a number of reports

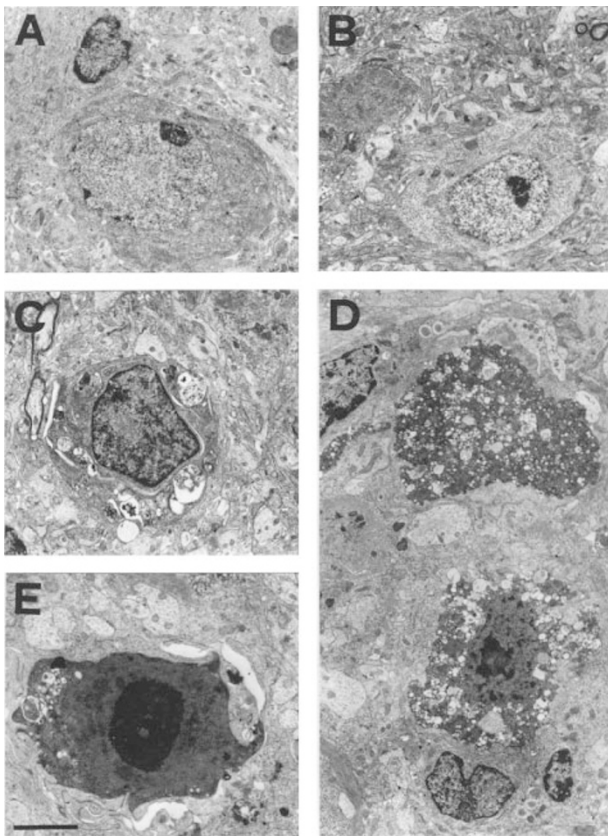


Figure 7 Electron microscopic evidence for apoptotic cell death in organotypic hippocampal slices exposed to 30 min OGD. (A) Control neuron showing a large nucleus with dispersed chromatin, a well defined nucleolus, and a cytoplasm rich in organelles. (B) A neuron observed 6 h after OGD, appearing still normal and healthy. (C) Another neuron observed 6 h after OGD, showing apoptotic signs of neurodegeneration. Clumps of chromatin are visible, as well as an electron-dense cytoplasm containing a number of vacuoles with non-homogeneous content. (D) Two neurons, observed 24 h after OGD, are undergoing apoptosis, as shown by their electron-dense cytoplasm containing numerous vacuoles. The neuron at the bottom has a highly condensed, shrunken nucleus. Surrounding glial cells appear unaltered. (E) In a section at higher magnification 24 h after OGD, an extremely condensed apoptotic body with a few vacuoles is visible, encircled by glial cell processes. Bar = 3 μm (A–D) and 2 μm (E)

showing that reduction of PARP activity by means of pharmacological or gene targeting strategies does not protect neuronal^{39,40} or non-neuronal^{41–43} cells against a variety of deleterious insults.

Because excitotoxicity, which is thought to occur by necrosis,⁴⁴ is an important component of ischemic neuronal death, a contribution of apoptosis was initially excluded in hypoxia-ischemia. More recently, features of both necrosis and apoptosis have been found in neurons after ischemic insults. Most investigators presently favor the view that programmed cell death and excitotoxicity are triggered in parallel in ischemic tissue, leading to a mosaic of morphological, and even biochemical, features.^{33–35,45–47} The occurrence or the prevalence of necrotic or apoptotic cell death in ischemic models depends on a number of factors including the intensity and the duration of the stimulus, the brain region and the type of cell involved,

and the developmental stage and functional status of the neurons. In this study, evidence for apoptotic-like features included the following: increased caspase-3-like activity, neuroprotection with a caspase inhibitor, presence of fragmented apoptotic nuclei stained by Hoechst 33258, terminal deoxynucleotidyl transferase (TdT)-mediated DNA end-labeling with fluorescent deoxynucleotides, and the detection of apoptotic neurons and bodies by electron microscopy. All these methods produced concordant results, indicating that apoptosis contributes to neuronal death following OGD in organotypic hippocampal slices but not in cortical cell cultures. In order to avoid the possible obfuscation of apoptosis by secondary necrosis,³⁷ cortical cells were examined at various time points after the insult, which revealed a time-dependent release of LDH into the medium and the appearance of ultrastructural features of necrotic cell death. Neither caspase-3 activation nor morphological characteristics of apoptosis could be observed in this experimental model at any time point after OGD, confirming previous studies showing that OGD-induced injury in cortical cells leads to excitotoxic necrosis with no evidence of apoptosis.⁴⁸ In contrast, a marked increase in caspase-3 activity was observed in organotypic hippocampal slices after OGD, together with morphological evidence of apoptotic neuronal death in the CA1 subregion and reduction of CA1 pyramidal cell death by use of the caspase inhibitor Z-VAD-FMK. Similar results with a different caspase inhibitor have been recently obtained in the same experimental model.⁴⁹ At the ultrastructural level, apoptotic neurons were evident at 6 and 24 h after OGD. These results are somewhat in contradiction with those of a recent study where the type of cell death was judged to be necrotic, instead of apoptotic, 24 h after OGD in hippocampal slices.⁵⁰ We cannot explain this discrepancy, although it may depend on differences in the experimental protocols. It is worth noting, however, that the use of a number of alternative approaches confirmed our electron microscopy observations suggesting an involvement of apoptosis in this experimental model.

Our results suggest that PARP overactivation is involved in post-ischemic injury only when necrosis accounts for most of the neuronal death. Similar conclusions have been reached by investigations using fibroblasts⁴³ or transplanted mesencephalic neurons⁴⁰ from PARP-deficient mice. A consistent relationship between PARP activation and necrosis but not apoptosis has also been reported for a number of apparently conflicting results obtained in PARP deletion or inhibition studies.⁴³ For example, pharmacological and genetic inhibition of PARP is neuroprotective in stroke models,^{16,17} where the massive pan-cellular death of the lesion core is unequivocally necrotic.^{51,52} However, morphological features of apoptosis⁵³ and neuroprotection with interventions that selectively block the apoptotic cascade^{54–56} have also been described in focal ischemia, especially in the penumbral area or when the infarction evolves in a delayed fashion.⁵⁷ It therefore appears that apoptosis may be revealed under particular conditions in focal ischemia *in vivo*, similarly to what

occurs in cortical cells *in vitro*, where apoptotic death can be unmasked by extending the OGD exposure to >90 min combined with the blockade of the excitotoxic component of OGD-induced neuronal death using ionotropic glutamate receptor antagonists.^{58,59} Interestingly, the brain tissue of mice protected against middle cerebral artery occlusion by genetic or pharmacological inhibition of PARP displays no change in apoptotic markers as compared with ischemic controls,¹⁹ further suggesting that PARP activation mediates only the necrotic component of focal ischemic injury. We have not examined the necrotic or apoptotic features of CA1 pyramidal cell injury following global ischemia in the gerbil, but previous studies have shown that cell death in this model can coexist as apoptosis,^{60–62} necrosis⁶³ and hybrid forms along an apoptosis-necrosis continuum.³³ Taking our results together with these literature findings, it is tempting to suggest that data obtained in cultured cortical cells may be predictive of events occurring in focal ischemia, whereas OGD exposure in organotypic hippocampal slices may trigger processes that are similar to those evoked in global ischemia.

PARP may be transiently activated in the early phases of apoptosis,⁶⁴ but soon after the protein is cleaved and inactivated by caspase-3.^{36,65} PARP cleavage in apoptosis is thought to prevent ATP depletion by PARP overactivation, preserving ATP and thus affording the energy required for the apoptotic active process. On the contrary, PARP overactivation leads to ATP intracellular depletion and energy deficit in necrotic cell death. It has been demonstrated that PARP activation determines the mode of cell death by regulating the intracellular levels of ATP and that ATP depletion can transform an ongoing apoptotic process into necrosis.^{66,67} Along this line, PARP activation appears to be required for necrosis, suggesting that poly(ADP-ribosylation) may be regarded as an active step in this cell death pathway.⁴³ PARP inhibitors may therefore be of therapeutic importance in brain pathologies where necrosis predominates.

Materials and Methods

Materials

DPQ was synthesized starting from 4-hydroxy-indan-1-one, which was submitted to a Schmidt reaction to give 5-hydroxy-isoquinolin-1(2H)-one. A sequential reaction with 1,4-dichlorobutane under phase transfer conditions and piperidine then led to DPQ. Benzamide, glutamate and PND were purchased from Sigma-Aldrich (Milan, Italy), NBQX was from Tocris Cookson (Bristol, UK), and Z-VAD-FMK was from Calbiochem (La Jolla, CA, USA). [Adenine-2,8-³H]NAD (1.5 Ci/mmol) was from Du Pont/NEN (Milan, Italy). LDH activity was quantified using the Cytotoxicity Detection Kit (LDH) from Roche Diagnostics (Monza, MI, Italy). Hoechst 33258 (bis-benzimide), propidium iodide (PI) and the EnzChek™ Caspase-3 Assay Kit #2 were purchased from Molecular Probes Europe (Leiden, The Netherlands). The Fluorescein-FragEL™ DNA Fragmentation Detection Kit was from Oncogene Research Products (Cambridge, MA, USA).

Partial purification and measurement of PARP activity *in vitro*

PARP was extracted and purified from the neonatal calf thymus according to Ito *et al.*⁶⁸ Briefly, a total of approximately 1 g (wet weight) of thymus was homogenized in 4 vol of a buffer containing 50 mM Tris-HCl (pH 8.0), 0.3 M NaCl, 10% glycerol, 10 mM 2-mercapto-ethanol, and 50 mM sodium bisulfite. After centrifugation (12 000 × g, 5 min), 150 μl of a 3.75% protamine sulfate solution was added to the supernatant while gently stirring on ice for 5 min. After brief centrifugation, the crude extract was applied on a DNA-agarose affinity chromatography column (25 × 0.5 cm; 0.7 mg DNA/ml of bed volume of 4% agarose) and then eluted with 1.2 M NaCl. PARP activity was assayed in active fractions according to Banasik *et al.*²⁶ The reaction mixture (100 μl) containing 100 mM Tris-HCl (pH 8.0), 20 mM MgCl₂, 5 mM dithiothreitol, 20 μg calf thymus sonicated DNA, 0.2 μCi [adenine-2,8-³H]NAD, and 60 μl of partially purified enzyme preparation was incubated at 37°C for 30 min. The reaction was terminated by adding 50% trichloroacetic acid and the radioactivity incorporated from [adenine-2,8-³H]NAD into proteins was evaluated by liquid scintillation spectrometry.

Oxygen-glucose deprivation in cortical cell cultures

Primary cultures of mixed cortical cells containing both neuronal and glial elements were prepared as previously described.⁶ Cerebral cortices were dissected from fetal mice at 14–15 days of gestation, minced using medium stock [MS, composed of Eagle's Minimal Essential Medium (MEM, with Earle's salts, glutamine- and NaHCO₃-free, GIBCO-BRL, San Giuliano Milanese, Italy) supplemented with 38 mM NaHCO₃, glucose (final concentration 22 mM), 100 units/ml penicillin and 100 μg/ml streptomycin], and then incubated for 10 min at 37°C in MS supplemented with 0.25% trypsin and 0.05% DNase. Enzymatic digestion was terminated by a second incubation (10 min at 37°C) in MS supplemented with 10% heat-inactivated horse serum and 10% fetal bovine serum, following which the cells were mechanically disrupted and counted. After brief centrifugation, cells were suspended at a density of approximately 4 × 10⁵ cells/ml and plated in 15 mm multiwell vessels on a layer of confluent astrocytes using a plating medium of MS supplemented with 10% heat-inactivated horse serum, 10% fetal bovine serum, and 2 mM glutamine. Cultures were kept in an incubator at 37°C, 100% humidity, and 95% air/5% CO₂ atmosphere. After 4–5 days *in vitro* (DIV), non-neuronal cell division was halted by the application of 3 μM cytosine arabinoside for 24 h. Cultures were then shifted to a maintenance medium identical to the plating medium but lacking fetal bovine serum, which was then partially replaced twice a week. Experiments were performed with mature cultures (14–15 DIV).

OGD was induced in mixed cortical cultures as described.⁶ The culture medium was replaced by thorough exchange with a glucose-free balanced salt solution (composition, in mM: 116 NaCl, 5.4 KCl, 0.8 MgSO₄, 1 NaH₂PO₄, 26 NaHCO₃, 1.8 CaCl₂, 10 mg/L phenol red) which had previously been saturated with 95% N₂/5% CO₂ and heated to 37°C. Multiwells were then sealed into an airtight incubation chamber equipped with inlet and outlet valves and 95% N₂/5% CO₂ was blown through the chamber for 10 min to ensure maximal removal of oxygen. The chamber was then sealed and placed into the incubator at 37°C for 60 min. OGD was terminated by removing the cultures from the chamber, replacing the exposure solution with oxygenated MS, and returning the multiwells to the incubator under normoxic conditions. The extent of neuronal death was assessed 24 h later. In order to achieve a maximal degree of neuronal injury, mixed cortical

cultures were exposed for 24 h to a high concentration (1 mM) of glutamate in MS at 37°C, 100% humidity and 95% air/5% CO₂ atmosphere.

Oxygen-glucose deprivation in organotypic hippocampal slices

Organotypic hippocampal slice cultures were prepared as previously reported.⁶ Briefly, the hippocampi were removed from the brain of 7-day-old Wistar rats and transverse slices (420 μm) were prepared using a McIlwain tissue chopper in a sterile environment. Isolated slices were first placed into ice-cold Hanks' balanced salt solution (HBSS, ICN Pharmaceuticals, Opera, MI, Italy) supplemented with 5 mg/ml glucose and 1.5% Fungizone[®] (GIBCO-BRL) and then transferred to humidified semiporous membranes (30 mm Millicell-CM 0.4 μm tissue culture plate inserts, Millipore, Rome, Italy; 4 per membrane). These were placed in 6-well tissue culture plates containing 1.2 ml of culture medium containing 50% Eagle's MEM (ICN Pharmaceuticals), 25% heat-inactivated horse serum, 25% HBSS, 5 mg/ml glucose, 1 mM glutamine and 1.5% Fungizone[®]. Slices were maintained at 37°C, 100% humidity, and 95% air/5% CO₂ atmosphere and the medium was changed every 4 days. Experiments were carried out after 14 DIV.

OGD was induced in organotypic hippocampal cultures as previously described in detail.⁶ Slices were preincubated for 30 min in serum-free medium and then subjected to OGD by exposing them to a serum-free medium devoid of glucose and previously saturated with 95% N₂/5% CO₂. Following 30 min incubation at 37°C in the airtight anoxic chamber, the cultures were transferred to oxygenated serum-free medium containing 5 mg/ml glucose and 5 μg/ml PI and returned to the incubator under normotoxic conditions until neuronal injury was evaluated 24 h later. Maximal damage was achieved in this system by exposing the slices for 24 h to 10 mM glutamate in the incubator using serum-free medium.

Assessment of neuronal injury *in vitro*

Cell damage in mixed cortical cultures was quantitatively evaluated by measuring the amount of LDH released from injured cells into the extracellular fluid 24 h following exposure to OGD or glutamate, as previously described.⁶ The LDH level corresponding to complete neuronal death (without glial death) was determined for each experiment by assaying sister cultures exposed to 1 mM glutamate for 24 h. Background LDH release was determined in control cultures not exposed to OGD and was subtracted from all experimental values. The resulting value correlated linearly with the degree of cell loss estimated by observation of cultures under phase-contrast microscopy or under bright-field optics following 5 min incubation with 0.4% trypan blue, which stains debris and nonviable cells.

Cell injury was assessed in organotypic hippocampal cultures using PI, a polar dye which enters the cells only if the membrane is damaged and becomes fluorescent upon binding to DNA.⁶ PI fluorescence was viewed using an Intracellular Imaging Inc. (Cincinnati, OH, USA) imaging system, consisting of a Xenon-arc lamp, a Nikon TMS-F inverted microscope equipped with a Groony[™] fluorescence optics module for epi-illumination, a low power objective (4×), and a rhodamine single-wavelength filter set (Omega Optical)-5727). Images were digitized using a video image obtained by a CCD camera controlled by software (InCyt Im1[™], Intracellular Imaging Inc.) and subsequently analyzed using the Image-Pro Plus morphometric analysis software (Media Cybernetics, Silver Spring, MD, USA). In order to quantify cell death, the CA1 hippocampal subfield was identified under phase-contrast optics and encompassed by a frame

using the drawing function in the image software. PI fluorescence was then collected without moving the tissue culture plate mounted on the microscope stage. A PI fluorescence intensity measurement for any given subfield consisted of the mean of the fluorescence intensity values of each pixel in the area defined by the frame. Previous experiments,^{6,27} as well as a number of studies using organotypic hippocampal slices exposed to ischemia-related insults,^{69–73} have shown that there is a linear correlation between relative PI fluorescence and the number of injured cells as detected by morphological criteria. Percentage of cell death in each experiment was expressed as: % death = 100 (F₂₄ - F_B) / (F_{max} - F_B),⁷² where F₂₄ is subfield fluorescence 24 h after exposure to OGD, F_B is background PI fluorescence determined in control slices, and F_{max} is maximal fluorescence after complete neuronal death induced by 24 h exposure to 10 mM glutamate. In some experiments, mixed cortical cell cultures were incubated with 3.5 μg/ml PI for 20 min at 37°C following exposure to OGD and then observed as described above but with a 10× power epifluorescence objective.

Transient global ischemia and assessment of CA1 pyramidal cell injury in gerbils

Gerbils were exposed to transient ischemia as previously described.²⁹ Briefly: the animals were anesthetized with a mixture of 2% halothane, 75% nitrogen and 20% oxygen. Through a ventral midline neck incision, both common carotid arteries were isolated and occluded for 5 min using micro-arterial clamps. At the end of the occlusion period, the clamps were released allowing restoration of carotid blood flow and the incision was sutured. Body temperature was monitored and maintained at 37°C with a rectal thermistor and heating pad until the animals had fully recovered from anesthesia. Seven days after the ischemic insult, the gerbils were sacrificed by decapitation, their brains rapidly removed and frozen in dry ice. Coronal sections (20 μm) were cut in a cryostat and stained with toluidine blue. At least four microscopic sections for each animal were analyzed. Hippocampal injury was assessed quantitatively by counting the number of CA1 pyramidal cells appearing histologically normal. The experimental protocol was carried to the Italian guidelines for animal care (DL 116/92) in application of the European Communities Council Directive (86/609/EEC) and was formally approved by the Animal Care Committee of the Department of Pharmacology of the University of Florence.

Drug administration protocols

Stock solutions of PARP inhibitors were prepared for the *in vivo* OGD experiments by dissolving benzamide at 500 mM in balanced salt solution, DPQ at 10 mM in a solution containing 2.5% ethanol, 0.5% dymethyl sulfoxide and 1% HCl, and PND at 100 mM in dimethylformamide. Drugs were then diluted in balanced salt solution and added to the incubation medium of cortical cell and organotypic hippocampal cultures during the OGD insult and the subsequent 24 h recovery period.

For the *in vivo* global ischemia experiments, benzamide was dissolved in saline and DPQ and NBQX in 100% dymethyl sulfoxide and then injected intraperitoneally in a volume of 50 μl. Controls received an equal amount of vehicle. Three 30 mg/Kg *i.p.* injections of the AMPA receptor antagonist NBQX were administered at 0, 15 and 30 min after reperfusion. Because in preliminary experiments single doses of benzamide and DPQ failed to show a protective effect and the half-life of the compounds is unknown, three multiple injection paradigms were selected. Protocol 1 consisted of two injections (2 h before and 2 h after bilateral carotid occlusion) of either benzamide at 160 mg/Kg or DPQ at 10 mg/Kg, and was very similar to protocols

previously used for benzamide³¹ and DPQ²² in neuroprotection studies in rodents. Protocol 2 consisted of three injections of either benzamide at 60 mg/Kg or DPQ at 20 mg/Kg within 30 min post-ischemia (at 0, 15 and 30 min following reperfusion) and protocol 3 of four injections of DPQ (at 10 or 30 mg/Kg) within 360 min post-ischemia (at 0, 60, 180 and 360 min following reperfusion). In a previous gerbil study, a late injection at 360 min following reperfusion proved to be crucial in order to obtain neuroprotection with (*m*-nitrobenzoyl)-alanine.³⁰

Measurement of caspase-3 like activity

The EnzChek™ Caspase-3 Assay Kit #2 was used to measure increases in caspase-3 and other Asp-Glu-Val-Asp (DEVD)-specific protease activities in cortical cultures and organotypic hippocampal slices. The assay is based on the use of a bisamide derivative of rhodamine 110, containing DEVD peptides covalently linked to each of the dye amino groups, thereby suppressing its fluorescence. Upon enzymatic cleavage, the nonfluorescent bisamide substrate is converted in a two-step process to rhodamine 110, which exhibits fluorescent spectral properties similar to those of fluorescein. Mixed cortical cultures were harvested and washed in phosphate-buffered saline. After brief centrifugation, cell pellets were resuspended in lysis buffer (Component C) and incubated at 4°C for 30 min. Lysed cells were then centrifuged (5 min at 5000 r.p.m.) and the supernatants used to detect caspase-3 proteolytic activity. Organotypic hippocampal slices were washed with phosphate-buffered saline and exposed to the lysis buffer at 4°C for 10 min, with brief sonication. The resulting suspension was then centrifuged (5 min at 5000 r.p.m.) and the supernatants used for the enzymatic activity. The assay was performed by adding 50 µl of reaction buffer (Component D, final concentration: 10 mM PIPES, pH 7.4, 2 mM EDTA, 5 mM dithiothreitol, 0.1% CHAPS, and 50 µM benzyloxycarbonyl-DEVD-rhodamine 110 substrate) to 50 µl of the supernatants. After incubating the samples at room temperature for 30 min, fluorescence was measured with a fluorometer set at 496 nm excitation and 520 nm emission. Data were calculated as pmoles of rhodamine 110/10⁶ cortical cells or hippocampal slice.

Microscope analysis of cell necrosis and apoptosis

Nuclear morphological features of necrotic and apoptotic degeneration were analyzed by fluorescence microscopy with the nuclear dye Hoechst 33258 (bis-benzimide). Mixed cortical cells were fixed with 4% paraformaldehyde for 30 min, washed in phosphate-buffered saline, and then incubated for 10 min at 37°C with 1 µg/ml Hoechst 33258. Similarly, organotypic hippocampal slices were fixed with 4% paraformaldehyde for 6 h, washed, removed from the membranes and mounted on slides, and then incubated with the dye for 15 min. After washing in phosphate-buffered saline, cells and slices were viewed for nuclear chromatin morphology in an Olympus IX50 fluorescence inverted microscope equipped with an Olympus WU filter set (excitation: 330–385 nm) and a 20× (for cortical cells) or 40× (for organotypic slices) objective. Normal cells were identified by intact round-shaped nuclei with diffuse fluorescence and necrotic cells by highly refringent smaller nuclei with uniformly dispersed chromatin. Because nuclear condensation is a feature of both necrosis and apoptosis, only cells displaying nuclear fragmentation and blebbing were considered apoptotic. In organotypic hippocampal slices, fragmented apoptotic nuclei were counted in three CA1 fields per slice, averaged, and expressed as mean number of apoptotic cells per field of at least six slices.

In a different set of experiments, the Fluorescein-FragEL™ DNA Fragmentation Detection Kit was used to detect apoptotic cells in organotypic hippocampal cultures. In the kit, terminal deoxynucleotidyl transferase (TdT) binds to exposed 3'-OH ends of DNA fragments generated in response to apoptotic signals and catalyzes the addition of fluorescein-labeled deoxynucleotides. Slices were fixed with 4% paraformaldehyde for 6 h, removed from the semiporous membranes and mounted on gelatin-coated slides. They were then washed in 20 mM Tris (pH 7.6)-buffered saline for 15 min, covered with a solution containing 2 µg/ml proteinase K in 10 mM Tris (pH 8.0) and incubated for 10 min. After washing again, slices were covered with TdT equilibration buffer for 30 min and then with the TdT labeling reaction mixture (containing TdT and the deoxynucleotides) for 1.5 h at 37°C. Slides were then washed and coverslips were applied. Fluorescence microscopy was carried out with the Intracellular Imaging Inc. imaging system using a 10× epifluorescence objective and a fluorescein single-wavelength filter set (Omega Optical O-5716). In preliminary experiments using a variety of stimuli (staurosporine, NMDA, OGD), the relative intensity of DNA fluorescence observed using the FragEL Fragmentation Detection Kit was proportional to the number of apoptotic cells identified with the nuclear dye Hoechst 33258.

For electron microscopy, cultures were directly fixed for 30 min at room temperature with a mixture of 2% formaldehyde and 2.5% glutaraldehyde in 0.1 M cacodylate buffer (pH 7.4). Cells or slices were removed from the culture dishes with a scraper, osmicated and embedded in Epon. Ultrathin sections were stained with uranyl acetate and lead citrate and observed in a Jeol 1010 (Tokyo, Japan) electron microscope at 80 kV.

Acknowledgements

This work was supported by grants from the University of Florence, the Italian Ministry of University and Scientific and Technological Research (Programma Cofinanziato MURST 1998), and SmithKline Beecham (Harlow, UK).

References

- Choi D (1990) Cerebral hypoxia: some new approaches and unanswered questions. *J. Neurosci.* 10: 2493–2501
- Meldrum B and Garthwaite J (1990) Excitatory amino acid neurotoxicity and neurodegenerative disease. *Trends Pharmacol. Sci.* 11: 379–387
- Olney JW (1990) Excitotoxic amino acids and neuropsychiatric disorders. *Annu. Rev. Pharmacol. Toxicol.* 30: 47–71
- Lipton SA and Rosenberg PA (1994) Excitatory amino acids as a final common pathway for neurological disorders. *N. Engl. J. Med.* 330: 613–622
- Nicoletti F, Bruno V, Copani A, Casabona G and Knoepfel T (1996) Metabotropic glutamate receptors: a new target for the therapy of neurodegenerative disorders? *Trends Neurosci.* 19: 267–271
- Pellegrini-Giampietro DE, Cozzi A, Peruginelli F, Leonardi P, Meli E, Pellicciari R and Moroni F (1999) 1-Amino-1,5-dicarboxylic acid and (S)-(+)-2-(3'-carboxybicyclo[1.1.1]pentyl)-glycine, two mGlu1 receptor-preferring antagonists, reduce neuronal death in *in vitro* and *in vivo* models of cerebral ischemia. *Eur. J. Neurosci.* 11: 3637–3647
- Coyle JT and Puttfarcken P (1993) Oxidative stress, glutamate and neurodegenerative disorders. *Science* 262: 689–695
- Pellegrini-Giampietro DE (1994) Free radicals and the pathogenesis of neuronal death: cooperative role of excitatory amino acids. In: Armstrong D (ed) *Free Radicals in Diagnostic Medicine: A Systems Approach to Laboratory Technology, Clinical Correlations and Antioxidant Therapy*, Plenum Press: New York pp. 59–71

9. Garthwaite J (1991) Glutamate, nitric oxid and cell-signalling in the nervous system. *Trends Neurosci.* 14: 60–67
10. Cusi C, Suzuki H, Milani D, Facci L, Menegazzi M, Vantini G, Kanai Y and Skaper SD (1994) Poly(ADP-ribose) polymerase: early involvement in glutamate-induced neurotoxicity in cultured cerebellar granule cells. *J. Neurosci. Res.* 39: 38–46
11. Zhang J, Dawson VL, Dawson TM and Snyder SH (1994) Nitric oxide activation of poly(ADP-ribose) synthetase in neurotoxicity. *Science* 263: 687–689
12. de Murcia and Ménessier-de Murcia J (1994) Poly(ADP-ribose)polymerase: a molecular nick sensor. *Trends Biochem. Sci.* 19: 172–176
13. Yamamoto H, Uchigata Y and Okamoto H (1981) Streptozotocin and alloxan induce DNA strand breaks and poly(ADP-ribose) synthetase in pancreatic islets. *Nature* 294: 284–286
14. Sims JL, Berger SJ and Berger NA (1983) Poly(ADP-ribose) polymerase inhibitors preserve nicotinamide adenine dinucleotide and adenosine 5'-triphosphate pools in DNA-damaged cells: mechanism of stimulation of unscheduled DNA synthesis. *Biochemistry* 22: 5188–5194
15. Schraufstatter IU, Hinshaw DB, Hyslop PA, Spragg RG and Cochrane CG (1986) Oxidant injury of cells. DNA strand-breaks activate polyadenosine diphosphate-ribose polymerase and lead depletion of nicotinamide adenine dinucleotide. *J. Clin. Invest.* 77: 1312–1320
16. Szabó C and Dawson VL (1998) Role of poly(ADP-ribose) synthetase in inflammation and ischemia-reperfusion. *Trends Pharmacol. Sci.* 19: 287–298
17. Pieper AA, Verma A, Zhang J and Snyder SH (1999) Poly(ADP-ribose) polymerase, nitric oxide and cell death. *Trends Pharmacol. Sci.* 20: 171–181
18. Ha HC and Snyder SH (2000) Poly(ADP-ribose) polymerase-1 in the nervous system. *Neurobiol. Dis.* 7: 225–239
19. Endres M, Wang Z-Q, Namura S, Waerber C and Moskowitz MA (1997) Ischemic brain injury is mediated by the activation of poly(ADP-ribose) polymerase. *J. Cereb. Blood Flow Metab.* 17: 1143–1151
20. Tokime T, Nozaki K, Sugino T, Kikuchi H, Hashimoto N and Ueda K (1998) Enhanced poly(ADP-ribose)ylation after focal ischemia in rat brain. *J. Cereb. Blood Flow Metab.* 18: 991–997
21. Takahashi K, Pieper AA, Croul SE, Zhang J, Snyder SH and Greenberg JH (1999) Post-treatment with an inhibitor of poly(ADP-ribose) polymerase attenuates cerebral damage in focal ischemia. *Brain Res.* 829: 46–54
22. Takahashi K, Greenberg JH, Jackson P, Maclin K and Zhang J (1997) Neuroprotective effects of inhibiting poly(ADP-ribose) synthetase on focal cerebral ischemia in rats. *J. Cereb. Blood Flow Metab.* 17: 1137–1142
23. Lo EH, Bosque-Hamilton P and Meng W (1998) Inhibition of poly(ADP-ribose) polymerase: reduction of ischemic injury and attenuation of N-methyl-D-aspartate-induced neurotransmitter dysregulation. *Stroke* 29: 830–836
24. Eliasson MJL, Sampei K, Mandir AS, Hurn PD, Traystman RJ, Bao J, Pieper A, Wang Z-Q, Dawson TM, Snyder SH and Dawson VL (1997) Poly(ADP-ribose) polymerase gene disruption renders mice resistant to cerebral ischemia. *Nat. Med.* 3: 1089–1095
25. Suto MJ, Turner WR, Arundel-Suto CM, Werbel LM and Sebolt-Leopold JS (1991) Dihydroisoquinolones: the design and synthesis of a new series of potent inhibitors of poly(ADP-ribose) polymerase. *Anticancer Drug Res.* 6: 107–117
26. Banasik M, Komura H, Shimoyama M and Ueda K (1992) Specific inhibitors of poly(ADP-ribose) synthetase and mono(ADP-ribose)transferase. *J. Biol. Chem.* 267: 1569–1575
27. Pellegrini-Giampietro DE, Peruginelli F, Meli E, Cozzi A, Albani Torregrossa S, Pellicciari R and Moroni F (1999) Protection with mGlu1 receptor antagonists in models of ischemic neuronal death: time-course and mechanisms. *Neuropharmacology* 38: 1607–1619
28. Sheardown MJ, Neilson EO, Hansen AJ, Jacobsen P and Honoré T (1990) 2,3-Dihydroxy-6-nitro-7-sulfamoyl-benzo(F)quinoxaline: a neuroprotectant for cerebral ischemia. *Science* 247: 571–574
29. Pellegrini-Giampietro DE, Cozzi A and Moroni F (1994) The glycine antagonist and free radical scavenger 7-Cl-thio-kynurenate reduces CA1 ischemic damage in the gerbil. *Neuroscience* 63: 701–709
30. Cozzi A, Carpenedo R and Moroni F (1999) Kynurenine hydroxylase inhibitors reduce ischemic brain damage: studies with (*m*-nitrobenzoyl)-alanine (mNBA) and 3,4-dimethoxy-[*N*-4-(nitrophenyl)thiazol-2yl]-benzenesulfonamide (RO 61-8048) in models of focal or global ischemia. *J. Cereb. Blood Flow Metab.* 19: 771–777
31. Cusi C, Chopin P and Marien M (1996) Benzamide, an inhibitor of poly(ADP-ribose) polymerase, attenuates methamphetamine-induced dopamine neurotoxicity in the C57B1/6N mouse. *Brain Res.* 735: 343–348
32. Cusi C, Colpaert F, Koek W, Degryse A and Marien M (1996) Poly(ADP-ribose) polymerase inhibitors protect against MPTP-induced depletions of striatal dopamine and cortical noradrenaline in C57B1/6 mice. *Brain Res.* 729: 264–269
33. Martin LJ, Al-Abdulla NA, Brambrink AM, Kirsch JR, Sieber FE and Portera-Cailliau C (1998) Neurodegeneration in excitotoxicity, global cerebral ischemia, and target deprivation: a perspective on the contributions of apoptosis and necrosis. *Brain Res. Bull.* 46: 281–309
34. Lipton P (1999) Ischemic cell death in brain neurons. *Physiol. Res.* 79: 1431–1568
35. Nicotera P, Leist M and Manzo L (1999) Neuronal cell death: a demise with different shapes. *Trends Pharmacol. Sci.* 20: 46–51
36. Wang KKW (2000) Calpain and caspase: can you tell the difference? *Trends Neurosci.* 23: 20–26
37. Bonfoco E, Krainc D, Ankarcrona M, Nicotera P and Lipton SA (1995) Apoptosis and necrosis: two distinct events induced, respectively, by mild and intense insults with N-methyl-D-aspartate or nitric oxid/superoxide in cortical cell cultures. *Proc. Natl. Acad. Sci. USA* 92: 7162–7166
38. Koh J-Y, Wie MB, Gwag BJ, Sensi SL, Canzoniero LMT, DeMaro JA, Csernansky C and Choi DW (1995) Staurosporine-induced neuronal apoptosis. *Exp. Neurol.* 135: 153–159
39. Leist M, Single B, Kunstle G, Volbracht C, Hentze H and Nicotera P (1997) Apoptosis in the absence of poly-(ADP-ribose) polymerase. *Biochem. Biophys. Res. Commun.* 17: 518–522
40. Kaminski Schierle GS, Hansson O, Ferrando-May E, Nicotera P, Brundin P and Leist M (1999) Neuronal death in nigral grafts in the absence of poly (ADP-ribose) polymerase activation. *NeuroReport* 10: 3347–3351
41. Bowes J and Thiemermann C (1998) Effects of inhibitors of the activity of poly (ADP-ribose) synthetase on the liver injury caused by ischemia-reperfusion: a comparison with radical scavengers. *Br. J. Pharmacol.* 124: 1254–1260
42. Oliver FJ, de la Rubia G, Rolli V, Ruiz-Ruiz MC, de Murcia G and Ménessier-de Murcia J (1998) Importance of poly(ADP-ribose) polymerase and its cleavage in apoptosis. Lesson from an uncleavable mutant. *J. Biol. Chem.* 273: 33533–33539
43. Ha HC and Snyder SH (1999) Poly(ADP-ribose) polymerase is a mediator of necrotic cell death by ATP depletion. *Proc. Natl. Acad. Sci. USA* 96: 13978–13982
44. Gwag BJ, Koh J-Y, DeMaro JA, Ying HS, Jacquin M and Choi DW (1997) Slowly triggered excitotoxicity occurs by necrosis in cortical cultures. *Neuroscience* 77: 393–401
45. Charriaut-Marlangue C, Aggoun-Zouaoui D, Represa A and Ben-Ari Y (1996) Apoptotic features of selective neuronal death in ischemia, epilepsy and gp120 toxicity. *Trends Neurosci.* 19: 109–114
46. Dirnagl U, Iadecola C and Moskowitz MA (1999) Pathobiology of ischemic stroke: an integrated view. *Trends Neurosci.* 22: 391–397
47. Lee J-M, Zipfel GJ and Choi DW (1999) The changing landscape of ischaemic brain injury mechanisms. *Nature* 399 (suppl.): A7–A14
48. Goldberg MP and Choi DW (1993) Combined oxygen and glucose deprivation in cortical cell culture: calcium-dependent and calcium-independent mechanisms of neuronal injury. *J. Neurosci.* 13: 3510–3524
49. Ray AM, Owen DE, Evans ML, Davis JB and Benham CD (2000) Caspase inhibitors are functionally neuroprotective against oxygen glucose deprivation induced CA1 death in rat organotypic hippocampal slices. *Brain Res.* 867: 62–69
50. Laake JH, Haug F-M, Wieloch T and Ottersen OP (1999) A simple in vitro model of ischemia based hippocampal slice cultures and propidium iodide fluorescence. *Brain Res. Protoc.* 4: 173–184
51. van Lookeren Campagne M and Gill R (1996) Ultrastructural morphological changes are not characteristic of apoptotic cell death following focal cerebral ischemia in the rat. *Neurosci. Lett.* 213: 111–114
52. Rosenblum WI (1997) Histopathological clues to the pathways of neuronal death following ischemia/hypoxia. *J. Neurotraum.* 14: 313–326
53. Linnik MD, Zobrist RH and Hatfield MD (1993) Evidence supporting a role for programmed cell death in focal cerebral ischemia in rats. *Stroke* 24: 2002–2008
54. Martinou J-C, Dubois-Dauphin M, Staple JK, Rodriguez I, Frankowski H, Missotten M, Albertini P, Talabot D, Catsicas S, Pietra C and Huarte J (1994) Overexpression of BCL-2 in transgenic mice protects neurons from naturally occurring cell death and experimental ischemia. *Neuron* 13: 1017–1030

55. Hara H, Friedlander RM, Gagliardini V, Ayata C, Fink K, Huang Z, Shimizu-Sasamata M, Yuan J and Moskowitz MA (1997) Inhibition of interleukin 1 β converting enzyme family proteases reduces ischemic and excitotoxic neuronal damage. *Proc. Natl. Acad. Sci. USA* 94: 2007–2012
56. Namura S, Zhu J, Fink K, Endres M, Srinivasan A, Tomaselli KJ, Yuan J and Moskowitz MA (1998) Activation and cleavage of caspase-3 in apoptosis induced by experimental cerebral ischemia. *J. Neurosci.* 18: 3659–3668
57. Du C, Hu R, Csernansky C, Hsu CY and Choi DW (1996) Very delayed infarction after mild cerebral ischemia: a role for apoptosis? *J. Cereb. Blood Flow Metab.* 16: 195–201
58. Gwag BJ, Lobner D, Koh J-Y, Wie MB and Choi DW (1995) Blockade of glutamate receptors unmasks neuronal apoptosis after oxygen-glucose deprivation in vitro. *Neuroscience* 68: 615–619
59. Gottron FJ, Ying HS and Choi DW (1997) Caspase inhibition selectively reduces the apoptotic component of oxygen-glucose deprivation-induced cortical neuronal cell death. *Mol. Cell. Neurosci.* 9: 159–169
60. Okamoto M, Matsumoto M, Ohtsuki T, Taguchi A, Mikoshiba K, Yanagihara T and Kamada T (1993) Internucleosomal DNA cleavage involved in ischemia-induced neuronal death. *Biochem. Biophys. Res. Commun.* 196: 1356–1362
61. Nitatori T, Sato N, Waguri S, Karasawa Y, Araki H, Shibana K, Kominami E and Uchiyama Y (1995) Delayed neuronal death in the CA1 pyramidal cell layer of the gerbil hippocampus following transient ischemia is apoptosis. *J. Neurosci.* 15: 1001–1011
62. Honkaniemi J, Massa SM, Breckinridge M and Sharp FR (1996) Global ischemia induces apoptosis-associated genes in hippocampus. *Mol. Brain Res.* 42: 79–88
63. Colbourne F, Sutherland GR and Auer RN (1999) Electron microscope evidence against apoptosis as the mechanism of neuronal death in global ischemia. *J. Neurosci.* 19: 4200–4210
64. Simbulan-Rosenthal CM, Rosenthal DS, Iyer S, Boulares AH and Smulson ME (1998) Transient poly(ADP-ribosyl)ation of nuclear proteins and role of poly(ADP-ribose) polymerase in the early stages of apoptosis. *J. Biol. Chem.* 273: 13703–13712
65. Nicholson DW and Thornberry NA (1997) Caspases: killer proteases. *Trends Biochem. Sci.* 22: 299–306
66. Eguchi Y, Shimizu S and Tsujimoto Y (1997) Intracellular ATP levels determine cell death fate by apoptosis or necrosis. *Cancer Res.* 57: 1835–1840
67. Leist M, Single B, Castoldi AF, Kuhnle S and Nicotera P (1997) Intracellular adenosine triphosphate (ATP) concentration: a switch in the decision between apoptosis and necrosis. *J. Exp. Med.* 185: 1481–1486
68. Ito S, Shizuta Y and Hayaishi O (1979) Purification and characterization of poly(ADP-ribose) synthetase from calf serum. *J. Biol. Chem.* 254: 3647–3651
69. Tasker RC, Coyle JT and Vornov JJ (1992) The regional vulnerability to hypoglycemia-induced neurotoxicity in organotypic hippocampal culture: protection by early tetrodotoxin or delayed MK-801. *J. Neurosci.* 12: 4298–4308
70. Newell DW, Barth A, Papermaster V and Malouf AT (1995) Glutamate and non-glutamate receptor-mediated toxicity caused by oxygen and glucose deprivation in organotypic hippocampal cultures. *J. Neurosci.* 15: 7702–7711
71. Strasser U and Fischer G (1995) Protection for neuronal damage induced by combined oxygen and glucose deprivation in organotypic hippocampal cultures by glutamate receptor antagonists. *Brain Res.* 687: 167–174
72. Abdel-Hamid KM and Tymianski M (1997) Mechanisms and effects of intracellular calcium buffering on neuronal survival in organotypic hippocampal cultures exposed to anoxia/aglycemia or to excitotoxins. *J. Neurosci.* 17: 3538–3553
73. Pringle AK, Iannotti F, Wilde GJC, Chad JE, Seeley PJ and Sundstrom LE (1997) Neuroprotection by both NMDA and non-NMDA receptor antagonists in vitro ischemia. *Brain Res.* 755: 36–46